Damage reconnaissance and seismic response prediction of an East Coast U.S. building subjected to 2011 Virginia Earthquake

Xin Chu[1], James Ricles[2], Shamim Pakzad[3], James Martin[4], Golnaz Shahidi[5]

[1]Graduate Research Assistant, Dept. of Civil and Environmental Engineering, Lehigh University, Bethlehem, PA 18015. Email: xic411@lehigh.edu
[2]Professsor, Dept. of Civil and Environmental Engineering, Lehigh University, Bethlehem, PA 18015. Email: jmr5@lehigh.edu
[3]Assisstant Professor, Dept. of Civil and Environmental Engineering, Lehigh University, Bethlehem, PA 18015. Email: pakzad@lehigh.edu
[4]Professor, Dept. of Civil and Environmental Engineering, Clemson University, Clemson, SC 29634. Email: jrmart@clemson.edu
[5]Graduate Research Assistant, Dept. of Civil and Environmental Engineering, Lehigh University, Bethlehem, PA 18015. Email: sgs310@lehigh.edu

ABSTRACT

During the 2011 Mineral, Virginia Earthquake the Smithsonian Institute Museum Support Center (MSC) sustained considerable structural damage. An in-depth study was conducted to investigate the behavior of MSC during this earthquake and its potential implication on seismic risk of East Coast U.S. structures. The damage sustained by this building is documented and it is observed that the severity of damage is not uniformly distributed in the floor plan. A finite element model is created to perform the seismic response prediction using recorded ground motions in order to explain the cause of structural damage. A field vibration test was conducted to capture the dynamic characteristics of the building which are in turn used to calibrate the finite element model. Results from seismic analysis reveal that the main reason for seismic damage is local soil amplification and combined torsional and translational effects due to an eccentric floor mass distribution relative to the center of rigidity (CR) of the floor plan.

INTRODUCTION

On 1:51 PM August 23, 2011, a magnitude 5.8 earthquake (USGS 2011) occurred in Mineral, Virginia. The 2011 Virginia Earthquake, with a maximum perceived intensity of VII (very strong) on the Mercalli intensity scale, is the largest earthquake to strike the Central and Eastern United States (CEUS) in 70 years (Hough 2012). Research shows that the earthquake occurred as a shallow reverse rupture comprising of three sub-events (Chapman 2013). The earthquake, although centered in central Virginia, was felt as far north as Canada and caused substantial damage to structures in the Washington D.C. Metro area that is about 90 miles away from the epicenter.

Among those structures, the Smithsonian Institute Museum Support Center (MSC) experienced significant structural as well as non-structural damage, and was subsequently closed for a period of time for inspection and repairs. Typical structural damage is reported by an ERRI reconnaissance team (Beavers et al. 2011). There exists a lack of understanding on what caused the damage to the structure during the earthquake. As the MSC represents typical museum warehouse construction based on the seismic design provision of the 1980s in this region, it's of value to conduct an in-depth investigation to assess its seismic behavior and performance during the Virginia earthquake and the implications on its vulnerability to future seismic hazards.

This paper presents the damage reconnaissance of the MSC and predicts its seismic response by means of a finite element analysis (FEA). Reasons for the observed structural damage are provided. Based on the study, some suggestions are made regarding the future seismic performance of this type of structure.

BUILDING DESCRIPTION

The MSC (Figure 1(a)) is located in Suitland, MD (about 6 miles southeast of Washington D.C.) and is a warehouse complex for storage, research and management of the off-display collections of the Smithsonian Institute. Occupying a total area of 700,000 square feet, the MSC consists of five "Pods" and Offices (see Figure 1(b)) that were constructed during various periods. The Pods, which function as artifacts storage, are one-story precast concrete frames with in-filled masonry walls. The Offices are 2-story in-filled masonry precast concrete frames that are connected to the top of the Pods by steel trusses (Figure 2(a)). Both the Pods and the Offices have double T-beams at their roof. Pods and Offices 1-4 were constructed from 1981 to 1983. Inside Pods 1 and 2, there is a 2-story steel mezzanine that was later added to the existing concrete structures in the 1980's. The mezzanine is anchored on the ground floor of the existing concrete structure. The mezzanine is designed and constructed to be structurally independent from the existing concrete frame, except that the two structures share the same foundation (Figure 2(a)). The lateral force resisting system (LFRS) of the mezzanines consists of steel concentrically braced frames with diagonal cross bracing in two orthogonal directions of the structure (Figure 2(b)). The diagonal bracing comprises of 2" by 0.5" A36 steel straps. The columns are HSS section with A500 steel while beams are W shape with A36 steel. The floor system of the mezzanine is constructed with cast in-place 6" thick concrete on top of metal decking supported by steel beams. A 2 inch gap exists between the perimeter edge of mezzanine floor slabs and the Pod outer masonry walls. In 2007, Pod 5 and Office 5 were added to the previous structure in an expansion project.

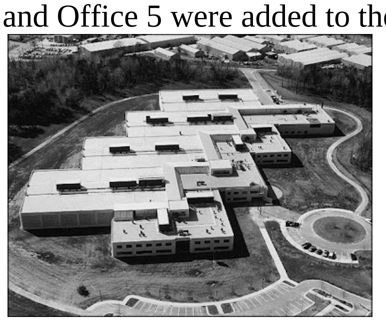

(a)

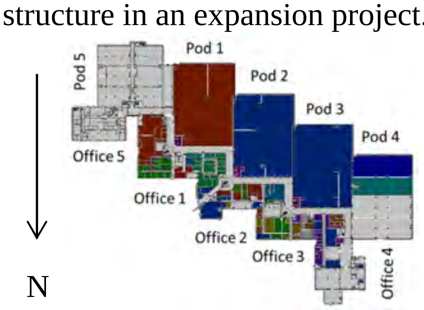

(b)

Figure 1. (a) Aerial view of MSC in 1980s (without Pod 5 and Offices 5) (www.mnh.si.edu); (b) Floor plan of MSC

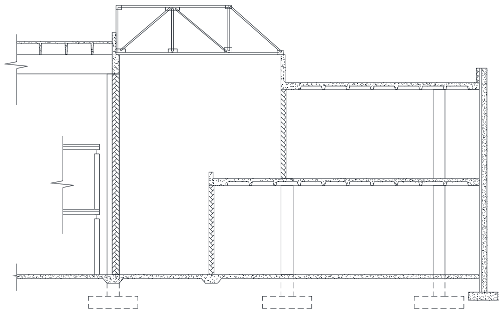

(a)

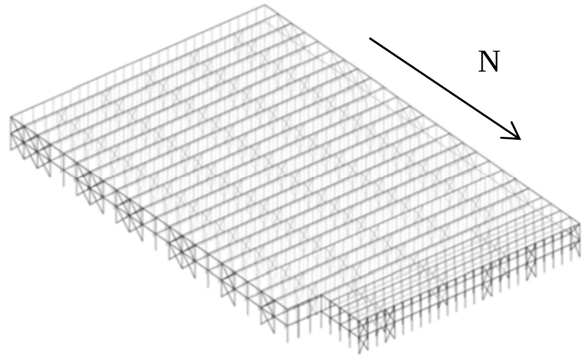

(b)

Figure 2. (a) Typical elevation of Pod, Offices and mezzanine; (b) Steel mezzanine inside Pod

DAMAGE TO MSC

The 2011 Virginia Earthquake caused extensive damage to both the concrete and steel frames of the MSC. The typical damage in the concrete structures includes concrete spalling, and cracking in the masonry wall and T-beam sliding (see Figure 3). Figure 3a shows a RC beam-column joint failure which is located in the corner of Office 1. In this specific failure, concrete at the ends of the beam and columns adjacent to the joint have spalled; the rebar has buckled; and the tile at the upper half of the corner has fallen off. Figure 3(b) shows a 2-inch sliding of a precast roof T-beam from its support bearing. Figure 3(c) shows a crack of about ¼” wide over the entire height of the masonry wall.

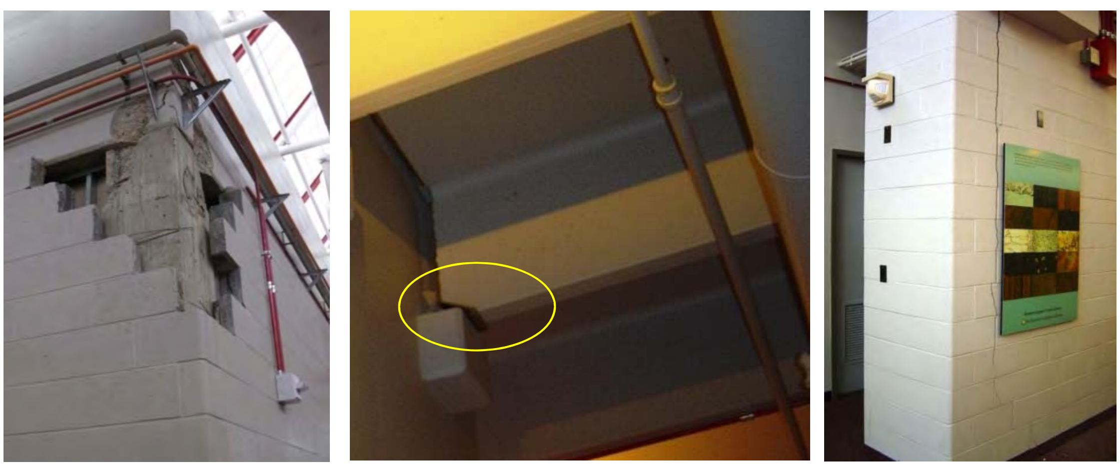

(a) (b) (c)

Figure 3. Representative damage in concrete and masonry structure: (a) RC beam-column joint failure; (b) sliding of reinforced concrete T-beam at roof; (c) cracking of CMU wall

Typical damage developed in the steel structure consisted of buckling, yielding and fracture of the diagonal bracing in both stories as well as column base plate anchor bolt failure at the ground floor. According to observations, the mezzanine in Pod1 suffered the most severe damage amongst all Pods. Damage occurred in both stories of the mezzanine but was more severe in the first story. The second story only suffered from some minor yielding and buckling. The condition and the locations of damage in the first story are illustrated in Figure 4.

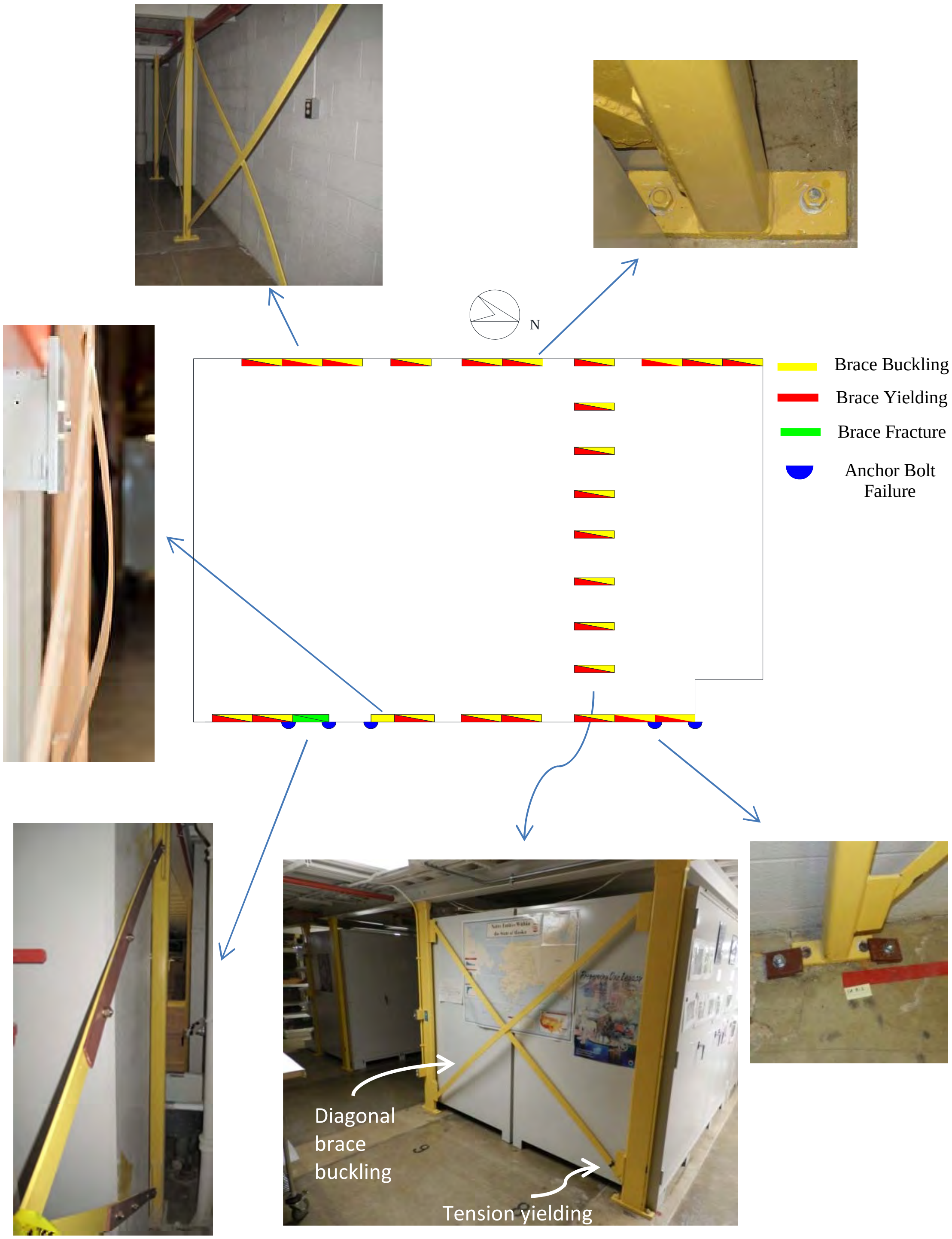

Figure 4. Type and distribution of damage in the first story of steel mezzanine in Pod 1

Several observations can be made:

1. The damage is associated with the diagonal bracing. Only the braces in the framing system were damaged and there is no observed damage in the beams or columns. Only the column base plate anchor bolts in the braced bays at the ground level are damaged.
2. Brace damage occurs only in the long direction of the floor plan of the mezzanine while those in the short direction remain intact.
3. Severity of damage is not uniformly distributed throughout the floor plan of the structure: the east perimeter of the structure is more seriously damaged. The extent of yielding or buckling of the diagonal braces in the east perimeter of the structure is more severe than that along the west perimeter. Moreover, in one braced bay along the east perimeter both of the cross bracing fractured at the first story. In addition, several column base plate anchor bolt failures occurred in the braced bays along the east perimeter while the anchor bolts in the west perimeters show no sign of damage.

FINITE ELEMENT MODELING OF MSC

The focus of this study is on the steel mezzanine in Pod 1, due to the severity and unique pattern of damage. FEA were performed to study the seismic behavior of the mezzanine during the Virginia Earthquake and investigate the cause of damage.

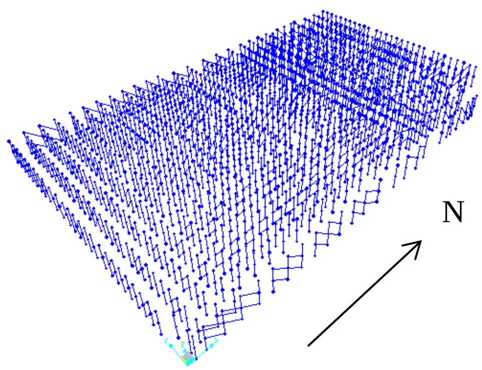

Figure 5. Isometric view of SAP2000 FEA model of steel mezzanine

A linear elastic finite element model is built using SAP2000 (Computers and Structures, Inc., 2010) (see Figure 5). The information obtained from the structural drawings is utilized to construct the model. The columns are modeled according to the structural drawings using beam-column elements. Due to the composite action of the floor slab, the beams are considered axially and flexurally rigid. Therefore, the structure is modeled as a shear building with the floor acting as a diaphragm. According to Metelli (2013), the effective slenderness ratio of the diagonal braces lies in the range of 594 to 1024, which corresponds to a compressive buckling stress of 0.27 to 0.81 ksi. As a result, the straps provide negligible compressive resistance during the earthquake and can be considered to be tension-only members. Therefore, only one of the crossing bracing members is modeled in the elastic SAP200 model within each braced bay to simulate the tension-only brace behavior. The mass of the structure is considered lumped at the center of mass (CM) at each floor level.

Although the structure behaved in a nonlinear manner during the earthquake, this linear model is used in the parametric time-history analysis. This is because the primary purpose of this model is to give a sense of which part of the structure may be potentially damaged and to identify the cause of structural damage. This linear elastic model facilitates this purpose for its fast computing time. In future fragility analysis, a nonlinear model will be constructed to capture the nonlinear behavior of the structure that occurs following the onset of damage.

FIELD TESTING AND MODEL VALIDATION

A field vibration test was conducted on the mezzanine to capture the modal property of the structure as a means to validate the structure. Both wired and wireless accelerometers were deployed around the second and third floor to measure the ambient vibrations. System identification algorithm in Chang and Pakzad (2013) is employed on measured acceleration time series to extract the modal property of the structure. Three vibration modes are identified. Table 1 presents the identified periods compared with analytical periods of model of Case I (explained in later sessions). The measured results have a better agreement with the as-built model when the compression is also modeled. The reason is that the behavior of the braces is amplitude dependent. At ambient vibration level, the amplitude of the vibration is low, thus the compressive braces won't buckle and can still provide stiffness. However, under earthquake excitation, the vibration amplitude is very large and the braces will buckle at very early stage and are not effective in providing compression resistance. So during earthquake excitation, it is reasonable to model the braces as tension-only while in ambient vibration tests the compression braces should also be considered. Each of these two models matches with their respective observation. Thus the model of Case I appears to perform better than models considered. In future analysis of the building, Case I model will be adopted.

Table 1 Comparison of measured and analytical period of different models (unit: s)

	Brace condition	Mode					
		1	2	3	4	5	6
Experimental	\	0.3	\	0.21	\	0.11	\
Analytical	Tension only	0.42	0.33	0.28	0.16	0.13	0.11
	As-built	0.32	0.25	0.21	0.12	0.10	0.08

PARAMETRIC STUDY AND INVESTIGATION OF CAUSE OF MSC STRUCTURAL DAMAGE

A major challenge to study the seismic behavior of MSC during the Virginia Earthquake is to account for the various structural uncertainties that affect its dynamic characteristic. Among them, is the effective seismic mass of the structure which presents the largest uncertainty.

The steel mezzanine is used to store the off-site artifacts of the museum. The storage cabinets constitute a significant portion of the total weight of the mezzanine. From a survey performed by the staff of the MSC the content weight inside the cabinets is estimated to range from 483.7 kips to 1802.1 kips for each floor while the self-weight of all the cabinets amounts to 632.3 kips per floor. The self-weight of the structure, including the floor slab and framing system, is 1770.8 kips per floor.

As there are more than 1000 cabinets on each floor, it will be prohibitively difficult to vary the weight of every cabinet to study the effect of content weight on the location of the floor mass. So instead, seven extreme representative cases of mass distribution are considered, and are shown in the floor plan provided in Figure 6. In Cases I, II and VII, all the cabinets have minimum, maximum and average content weight distributed uniformly over the floor plan of both floors, respectively. In Cases III and IV, the floor plan is trisected along its short direction (EW direction), with all the cabinets within each subarea having the same mass distribution. For example, in Case III, all the cabinets in the 2/3rds of the floor plan towards the east direction have the minimum mass while those in the lower 1/3 of the floor plan in the west direction have maximum mass. In Case V and VI, the floor plan is trisected along its long direction (NS direction), as shown in Figure 6(e) and (f).

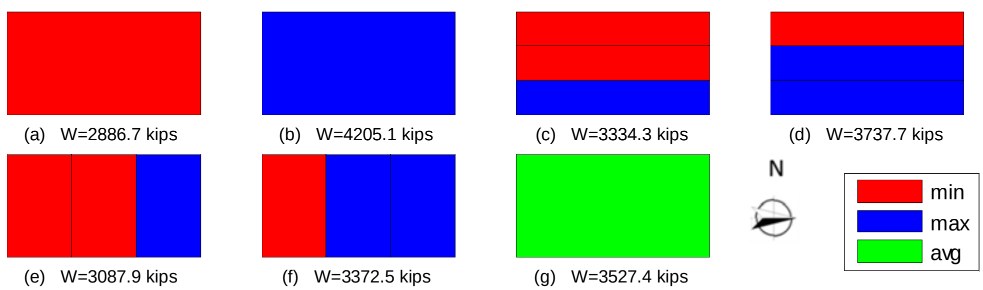

Figure 6. Illustration of cabinet content weight distribution and resultant total floor weight over floor plan: (a) Case I; (b) Case II; (c) Case III; (d) Case IV; (e) Case V; (f) Case VI; (g) Case VII

The location of the center of mass (CM) for each case of content weight and the center of rigidity (CR) are shown in Figure 7. A summary of the eccentricity between the CR and CM for each case is given in Table 2. The total floor weight and location of CM show a large variance due to a wide range of possible content weight.

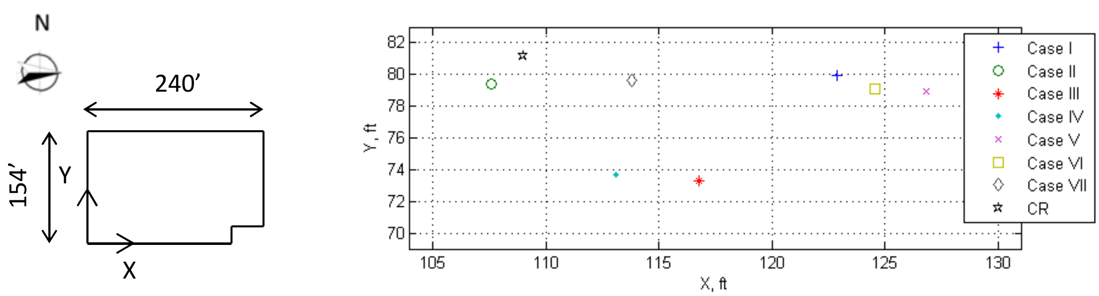

Figure 7. Location of the CM within the floor plan of the mezzanine for each cabinet content weight case

Table 2 Eccentricity between CR and CM (unit: ft)

	I	II	III	IV	V	VI	VII
NS	-13.9	1.4	-7.8	-4.1	-17.8	-15.5	-4.8
EW	1.2	1.8	7.9	7.6	2.2	2.1	1.6

Unfortunately, there is no recorded free-field ground motion in the DC region. Therefore the ground motions at the MSC are generated from ground motions that were recorded in Reston, VA. This process consists of conducting a deconvolution of the Reston surface ground motion into bed rock and then convoluting these motions up to ground surface of at the MSC utilizing measured soil profiles of the region. The detailed description of this method can be found in Shahidi et al. (2013).

The time-history and response spectrum of the ground motion at the bed rock and the ground surface in MSC (rotated to the orthogonal directions of the mezzanine) are shown in Figures 8 and 9. Due to the uncertainty in the measured soil profile, several assumptions were made about the transition of shear wave velocity from the bed rock to the deepest point in the soil column where the shear wave velocity can be measured. It can be observed that regardless of the assumption on the transition of the shear wave velocity, the spectral response of 0.1s to 1s is significantly amplified by the local soil condition. It appears that soil amplification is one of the reasons that caused structural damage to the MSC, for as will be explained below the natural periods of the MSC fall in this range.

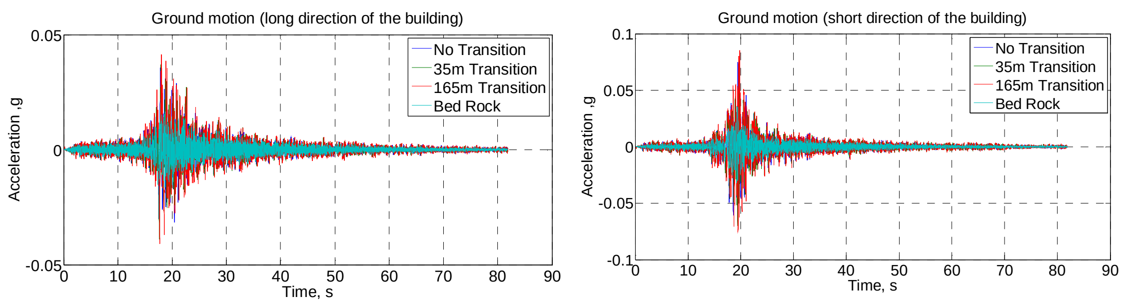

Figure 8. Time history of generated bi-directional ground motion at MSC

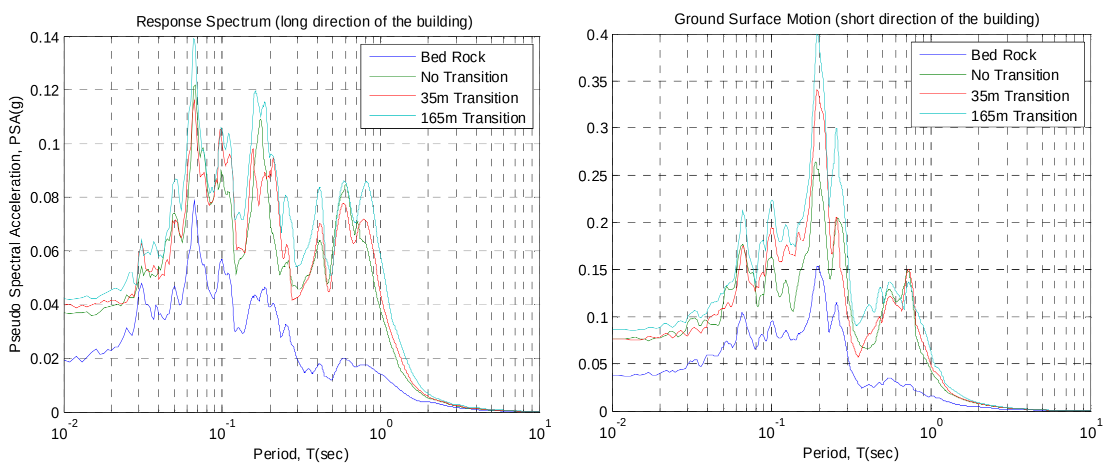

Figure 9. Response spectrum of generated bi-directional ground motion at MSC

The ground motion with the assumption of 165m of transition gives the largest response spectrum, and is therefore selected as the ground excitation applied to the structure in the parametric study. This study is performed by conducting time history analysis using the FE model and the above bi-directional ground motions. Different cases yield different results of seismic response. The result from Case I described in Figure 6 gives the closest agreement with the observed damage.

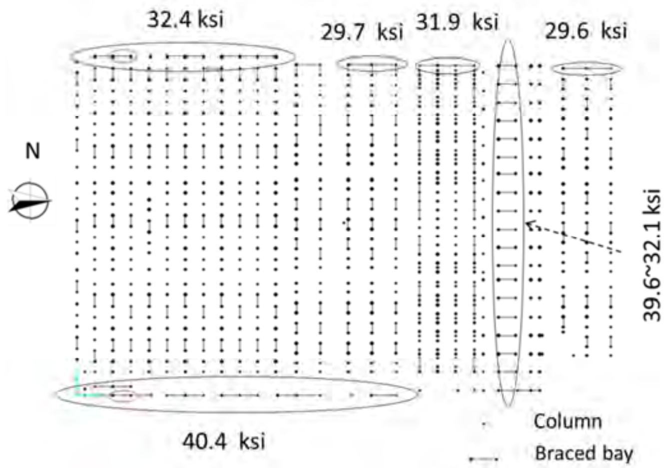

Figure 10. Peak axial stress response in 1st story braces, Case I

Figure 10 shows the peak axial tensile stress in the diagonal braces. The peak response is in the braces along the east perimeter, where the stress is as high as 40.4 ksi, exceeding the nominal yield stress of the 36 ksi (A36 steel). In comparison, the response of the diagonal braces along the west perimeter is smaller than their counterparts in the east perimeter. This is consistent with the observed damage pattern (Figure 4) in which the east perimeter of the structure suffered more damage than the west side.

By close examination, this unique damage pattern can be attributed to significant coupling between the translational and torsional displacement of the floor diaphragm induced by bi-directional ground motion excitation. The effect of bi-directional excitation is clearly demonstrated by comparing the response of the structure under uni-directional and bi-directional ground motion. Figure 11 presents the time-history of lateral displacement in the NS direction for two braced bays located respectively at the east and west perimeter (identified within the red circles in Figure 10) under uni-directional ground motion in the NS, EW and bi-directional ground motion, respectively. When the ground motion strikes in the EW direction (i.e., short direction of the building; Figure 11(b)), the displacement demand in the NS (i.e., long direction of the building) direction is comparable to the case when the building is subjected to ground motion in the NS direction (Figure 11(a)). In addition, the non-uniform response in braces in the long direction of the building is also caused by ground motion in the short direction of the building. The reason is, in this case, the CR of the first floor deviates from the CM by 13.9’ to the south and 1.2’ to the east (see Table 2). Larger eccentricity in the long direction creates a significant component of torsion in the second and third modes (Figure 13). In addition, the earthquake in the short direction has much larger magnitude than its perpendicular component, especially at the second and third modes due to the effect of soil amplification (Figure 12). Consequently, the torsional component from the second and third modes in response to the ground motion in the short direction will impose extra and non-uniform demand on the displacement response in the long direction.

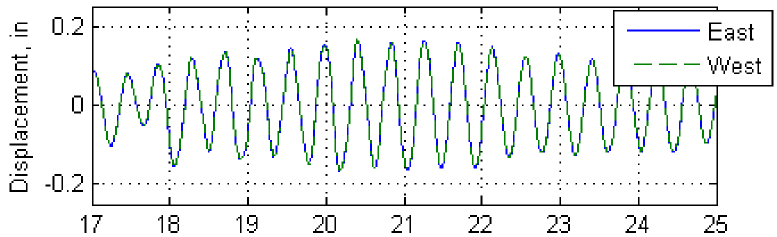

(a)

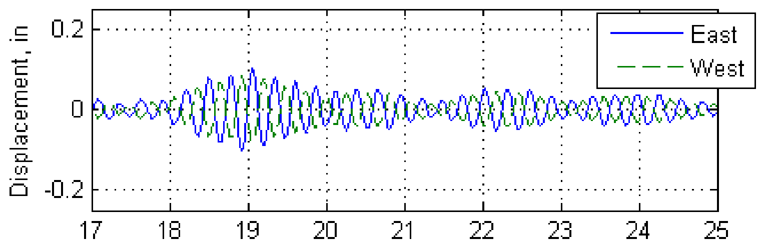

(b)

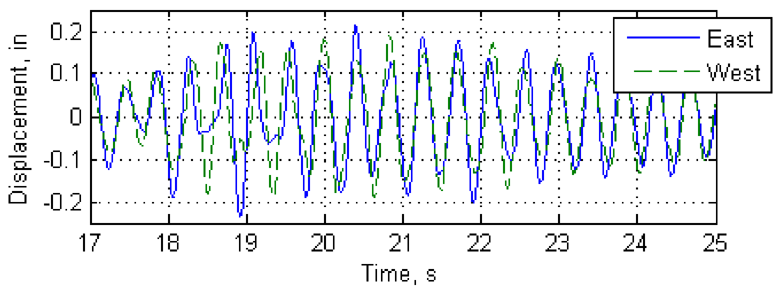

(c)

Figure 11. Time history for translation of joints at the top of columns in east and west perimeters: (a) response to ground motion in NS direction; (b) response to ground motion in EW direction; (c) response to bi-directional ground motion

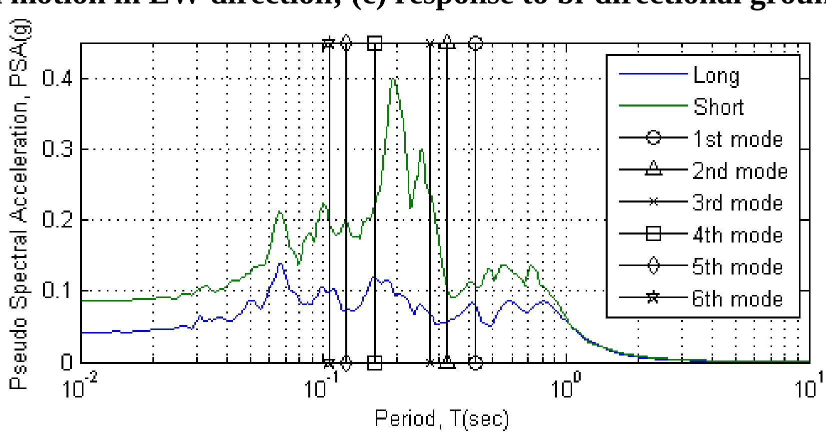

Figure 12 Response spectra of two components of ground motion and structural periods

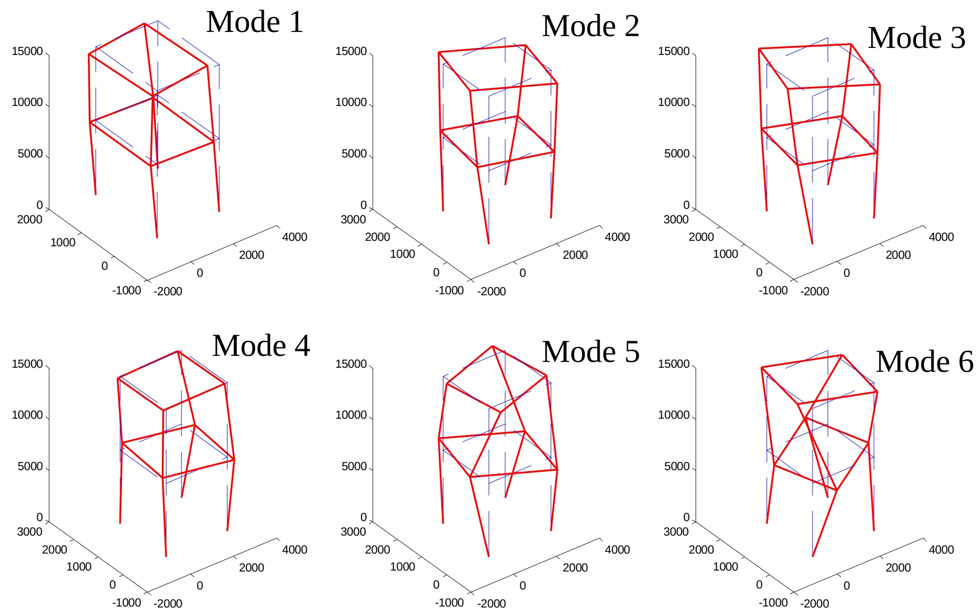

Figure 13 Mode shape of Case I model

SUMMARY AND CONCLUSIONS

Damage reconnaissance of the MSC was conducted following the 2011 Virginia Earthquake. For the steel mezzanine in Pod 1, a non-uniformed damage pattern was observed. A finite element model for the mezzanine was developed and calibrated using field vibration test data. Simulated ground motions were used to conduct time history analysis to predict the response of the structure during the Virginia Earthquake and investigate the cause of damage. The uncertainty associated with the structure is investigated through a parametric study of floor mass distribution. For one possible mass scenario, the predicted response by the finite element model shows good agreement with the observed damage pattern. In that case, the building is strongly coupled in torsion and translation. This effect, exacerbated by the bi-directional seismic demand, creates larger response in one perimeter of the structure than the other.

The causes of structural damage of steel mezzanine in Pod1 of MSC are

- Soil amplification
- Combined effect of torsion and translation response
- Bi-directional earthquake demand

This study also highlights the need to consider bi-directional ground motion excitation in seismic analysis and 3D modeling. For 3D structures, the seismic demand on lateral force resisting systems in one specific direction not only comes from ground motion in the same direction, but may also result from the ground motion in the perpendicular direction due to eccentricity between the CM and CR. Meanwhile, the demand on different parts of the structure may also be non-uniform.

Future work on fragility analysis of the structure considering bi-directional seismic demand and effect of eccentricity is underway using nonlinear finite element models.

ACKNOWLEDGEMENT

The research reported in this paper is supported by National Science Foundation Award No. CMMI-1219447. The authors are grateful for the staff at the Smithsonian Institute and the MSC for their help during several field visits. Special thanks go to Mr. Robert Kayen from USGS who provided measured soil profile data underneath the MSC. The support of DIGITEXX Data Systems who partially provided the wired instrumentation system is acknowledged.

REFERENCES

Beavers, J. E., Eatherton, M. R., Gilsanz, R. E., Ricles, J. M., Lin, Y. C. (2012). The August 23, 2011 Magnitude 5.8 Virginia Earthquake in the Eastern United States - An Engineering Perspective, Proceedings of 15th World Conference on Earthquake Engineering, Lisbon. Portugal.

Chang, M., Pakzad, S., N. (Accepted 2013). Observer Kalman filter identification for output-only systems using Interactive Structural Modal Identification Toolsuite (SMIT), (ASCE) Journal of Bridge Engineering, In Press DOI: 10.1061/(ASCE)BE.1943-5592.0000530.

Chapman, M. C. (2013). On the Rupture Process of the 23 August 2011 Virginia Earthquake, Bulletin of the Seismological Society of America, 103, 613–628, 2013.

Computers and Structures, Inc., (2010) CSI Analysis Reference Manual For SAP2000 (Version 14.2.4)

Hough, S. E. (2012). Initial assessment of the intensity distribution of the 2011 Mw 5.8 Mineral, Virginia earthquake, Seismologist Research Letters, 83(4), 649–657

Metelli, G. (2013). Theoretical and experimental study on the cyclic behaviour of X braced steel frames, Engineering Structures, Vol. 46, pp763-773

Shahidi, S.G., Pakzad, S.N., Ricles, J.M., Martin, J.R., Olgun, C.G., and Godfrey, E.A. (Submitted October 2013). Behavior and Damage to the Washington National Monument during the 2011 Virginia Earthquake. Geological Society of America (GSA) Special Paper volume on “The August 23, 2011 Earthquake in Central Virginia and Its Significance for Seismic Hazards in Eastern North America”, Under Review.

U.S. Geological Survey, (2011a). Magnitude 5.8 — Virginia: Summary, http://earthquake. usgs.gov/earthquakes/eqinthenews/2011/se082311a/#summary